Near band edge anisotropic optical transitions in wide band gap semiconductor Cu_2ZnSiS_4

S. Levcenco,[1,a)] D. Dumcenco,[1,a)] Y. S. Huang,[1,b)] E. Arushanov,[2] V. Tezlevan,[2] K. K. Tiong,[3] and C. H. Du[4]
[1]*Department of Electronic Engineering, National Taiwan University of Science and Technology, Taipei 106, Taiwan*
[2]*Institute of Applied Physics, Academy of Sciences of Moldova, Chisinau, MD 2028, Moldova*
[3]*Department of Electrical Engineering, National Taiwan Ocean University, Keelung 202, Taiwan*
[4]*Department of Physics, Tamkang University, Tamsui 251, Taiwan*

(Received 15 April 2010; accepted 17 August 2010; published online 6 October 2010)

In this study, anisotropic near band edge transitions of Cu_2ZnSiS_4 single crystals grown by chemical vapor transport were characterized by using polarization-dependent absorption, piezoreflectance (PzR) and surface photovoltage (SPV) spectroscopy techniques at room temperature. The measurements were carried out on the as grown basal plane with the normal along [2 1 0] and the axis **c** parallel to the long edge of the crystal platelet. Analysis of absorption and SPV spectra reveal indirect allowed transitions for the absorption edge of Cu_2ZnSiS_4. The estimated values of indirect band gap are 2.97 eV and 3.07 eV, respectively, for $\mathbf{E}\perp\mathbf{c}$ and $\mathbf{E}\parallel\mathbf{c}$ polarization configurations. The polarization-dependent PzR and SPV spectra in the vicinity of the direct band gap of Cu_2ZnSiS_4 reveal features $E_{\perp}^{ex}$ and $E_{\parallel}^{ex}$ at around 3.32 eV and 3.41 eV for $\mathbf{E}\perp\mathbf{c}$ and $\mathbf{E}\parallel\mathbf{c}$ polarizations, respectively. Both features $E_{\perp}^{ex}$ and $E_{\parallel}^{ex}$ are associated with the interband excitonic transitions at point Γ and can be explained by crystal-field splitting of valence band. Based on the experimental observations, a plausible band structure near band edge of Cu_2ZnSiS_4 is proposed. © *2010 American Institute of Physics*. [doi:10.1063/1.3490219]

I. INTRODUCTION

Cu_2ZnSiS_4 belongs to the family of Cu-based quaternary chalcogenide compounds, Cu_2-II-IV-VI_4, crystallizing in the wurtz-stannite structure with space group $Pmn2_1$.[1–3] The structure of Cu_2ZnSiS_4 consists of alternating cation layers of mixed Zn and Si atoms separated by layers of Cu atoms. It is therefore derived from an ordering of the cations of the wurtzite cell. In this compound each sulfur atom has four nearest neighbor cation atoms (two copper atoms, one zinc, and a silicon atom) at the corners of the surrounding tetrahedron.[1–3] The material is of interest for its nonlinear optical properties[4,5] and potential for application in optoelectronics.[6] Despite its interesting optical properties and possible applications, up-to-date, only a few studies have been reported concerning the basic properties of Cu_2ZnSiS_4,[7,8] due to the difficulty of preparing suitable size, compositionally homogeneous, and high purity single crystals. Among those studies, some discrepancies have been reported. For example, Schleich and Wold[7] performed the first optical absorption study of Cu_2ZnSiS_4 and the optical band edge of this material was determined to be 3.25 eV, whereas a more recent study by Yao *et al.*[8] determined the material to be an indirect semiconductor with an indirect band gap of 3.04 eV.

In this paper, we report a detailed study of the near band edge anisotropic optical properties of Cu_2ZnSiS_4 single crystals. High quality single crystals of Cu_2ZnSiS_4 were grown by chemical vapor transport using iodine as the transport agent. The optical anisotropic effects parallel and perpendicular to the long axis **c** of the crystals were studied by polarization-dependent absorption, piezoreflectance (PzR) and surface photovoltage spectroscopy (SPS) techniques at room temperature. The measurements were carried out on the as grown basal plane with the normal along [2 1 0] and the axis **c** parallel to the long edge of the crystal platelet. The polarization-dependent indirect band edge and direct band edge excitonic transitions were determined. Base on the obtained results, a plausible band structure near band edge of Cu_2ZnSiS_4 is proposed.

II. EXPERIMENTAL

Single crystals of Cu_2ZnSiS_4 were grown by vapor transport of stoichiometric amounts of the elements with 5 mg iodine/cm^3 as the transport agent. Optimum crystal growth was achieved with the charge zone maintained at 850 °C and the growth zone at 800 °C. The transport process was carried out for a period of 14 days. Single crystals Cu_2ZnSiS_4 formed thin, greenish, blade shape up-to 10 $\times 1.5$ mm^2 in area and 300 μm in thickness [see Fig. 1(a)]. Figure 1(b) shows the Laue diffraction pattern taken along the normal of the as grown basal plane. Laue pattern displays a twofold asymmetry pattern. Analyzing the symmetry of Laue pattern confirms the formation of orthorhombic structure and reveal that the normal of the basal plane is [2 1 0] and the long edge of the crystal platelet is parallel to **c** axis. Figure 1(c) depicts the rocking curve (θ scan) in the vicinity of (210) normal peak. The full width at half maximum

[a)]Permanent address: Institute of Applied Physics, Academy of Science of Moldova, 5, Academiei str., MD-2028, Chisinau, Republic of Moldova.
[b)]Electronic mail: ysh@mail.ntust.edu.tw.

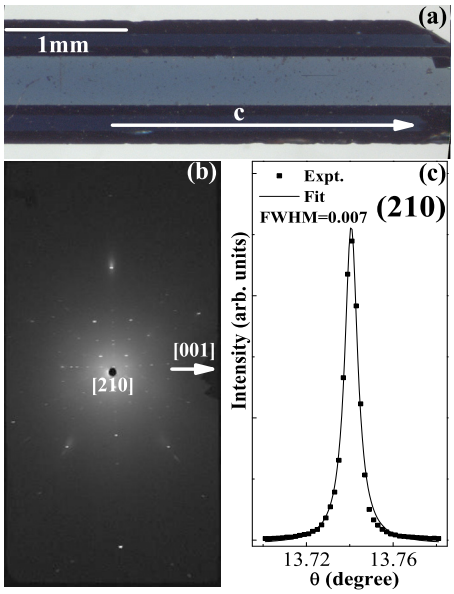

FIG. 1. (Color online) (a) Morphology of an as grown Cu_2ZnSiS_4 single-crystal with a scale bar, (b) the Laue diffraction pattern taken along the normal of the as grown basal plane, and (c) the rocking curve (θ scan) in the vicinity of (210) normal peak.

(FWHM) is determined to be 0.007°. The small value of FWHM indicates that high structural quality single crystals of Cu_2ZnSiS_4 were grown.

A 150 W xenon arc lamp filtered through by a 0.25 m grating monochromator provided the source for the optical measurements. Model PRH 8020 CASIX Rochon prisms were employed for polarization-dependent measurements. A model 3378 Hamamatsu photomuliplier tube was used to detect the transmitted or reflected signals. The PzR measurements were achieved by gluing the thin ($\sim$100 μm) single-crystal specimens on a 0.15 cm thick lead zirconate titanate piezoelectric transducer driven by a 300 V_{rms} sinusoidal wave at 200 Hz. The dc output of the reflected signal was maintained constant by a servomechanism of a variable neutral density filter. A dual-phase lock-in amplifier was used to measure the detected signals. In SPS measurements, the surface photovoltage (SPV) was measured between the sample and a reference metal grid electrode in a capacitive manner as a function of the photon energy of the probe beam. The intensity of the incident beam was normalized by a pyroelectric detector. The SPV spectrum on the metal grid was measured with a copper plate as the ground electrode, using a buffer circuit.

III. RESULTS AND DISCUSSION

The indirect band edge transitions of Cu_2ZnSiS_4 were studied by means of polarization-dependent absorption measurements. From polarization-dependent optical reflectivity and transmittance measurements, the absorption coefficient α of the sample crystals can be determined by using the relation[9,10]

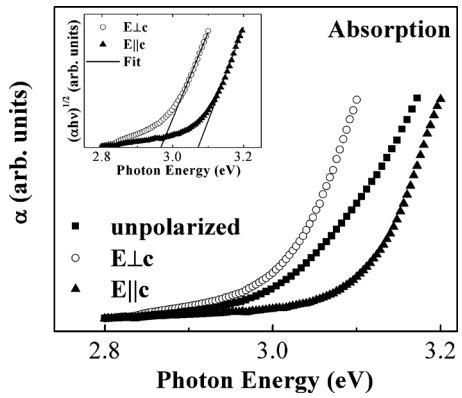

FIG. 2. The unpolarized, $\mathbf{E}\perp\mathbf{c}$ and $\mathbf{E}\|\mathbf{c}$ polarization absorption spectra of Cu_2ZnSiS_4 at room temperature. The inset illustrates the plots of $(\alpha h\nu)^{1/2}$ vs $h\nu$ for $\mathbf{E}\perp\mathbf{c}$ and $\mathbf{E}\|\mathbf{c}$ polarization in the vicinity of the indirect band gap.

$$T_r = \frac{(1-R)^2 e^{-\alpha d}}{1-R^2 e^{-2\alpha d}}, \tag{1}$$

where T_r represents the transmission coefficient, R is the reflectivity and d is the sample thickness. The reflectivity measurements were done on as grown basal surface and compared against an evaporated gold mirror. Figure 2 displays the absorption coefficient as a function of the photon energy for Cu_2ZnSiS_4 at room temperature. The open circles in Fig. 2 correspond to the $\mathbf{E}\perp\mathbf{c}$ polarization, the solid triangles represent $\mathbf{E}\|\mathbf{c}$ polarization and the solid squares are the unpolarized results. The polarization dependence of the absorption curves provides conclusive evidence that the two optical absorption edges are associated with interband transitions from different origins and the possible origins will be discussed later. It is noted that there is a residual absorption at photon energies below the absorption edge. For simplicity, the residual absorption is assumed to be a constant and subtracted out for the evaluation of the band gap.

It is well known that the band gap energy can be obtained by extrapolating the linear part of the plot $(\alpha h\nu)^n$ versus $h\nu$ to zero, where n equals to 2 for direct transitions and 1/2 for indirect allowed transitions, respectively.[11] As shown in Fig. 2, the absorption spectra obtained are fitted well using the relation $(\alpha h\nu)^{1/2}$ versus $h\nu$, which is the characteristic of indirect band structure. The inset of Fig. 2 illustrates an example of the process of extracting the indirect band gap values from the spectra of $\mathbf{E}\perp\mathbf{c}$ and $\mathbf{E}\|\mathbf{c}$ polarization configurations. The deduced values are summarized in Table I, where the indirect gaps for $\mathbf{E}\perp\mathbf{c}$ and $\mathbf{E}\|\mathbf{c}$ polarizations, denoted as $E_{g\perp}^{ind}$ and $E_{g\mathrm{II}}^{ind}$, are determined to be

TABLE I. Values of indirect band gaps and the excitonic transition energies of Cu_2ZnSiS_4 obtained from polarization-dependent absorption, PzR and SPS measurements at room temperature.

	Transitions			
Techniques	$E_{g\perp}^{ind}$ (eV)	$E_{g\mathrm{II}}^{ind}$ (eV)	$E_{\perp}^{ex}$ (eV)	$E_{\|}^{ex}$ (eV)
Absorption	2.97 ± 0.02	3.07 ± 0.02	⋯	⋯
PzR	⋯	⋯	3.322 ± 0.005	3.408 ± 0.005
SPS	2.99 ± 0.02	3.08 ± 0.02	3.32 ± 0.01	3.40 ± 0.01

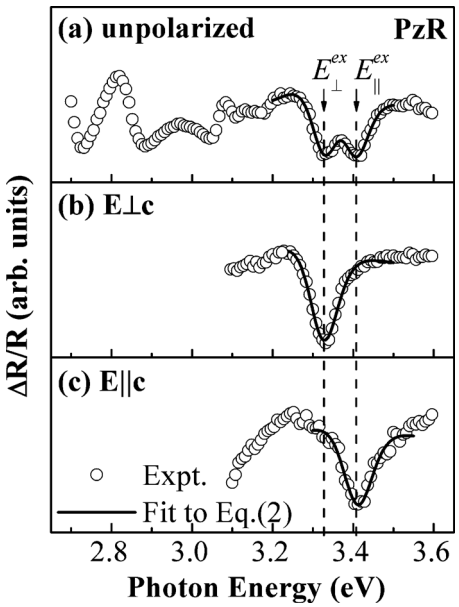

FIG. 3. The (a) unpolarized, (b) $\mathbf{E}\perp\mathbf{c}$ polarization, and (c) $\mathbf{E}\|\mathbf{c}$ polarization PzR spectra of Cu_2ZnSiS_4 at room temperature. The solid lines are least-squares fits of Eq. (2) to experimental data. The obtained values of the transition energies denoted as $E_{\perp}^{ex}$ and $E_{\|}^{ex}$ are indicated by the arrows.

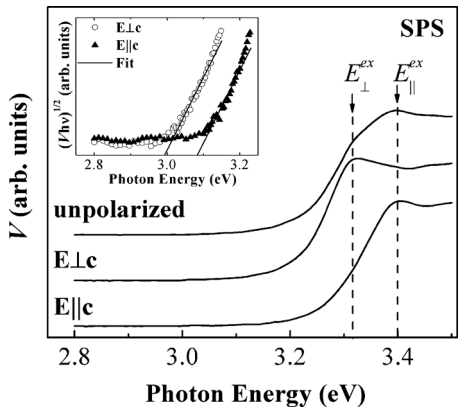

FIG. 4. The unpolarized, $\mathbf{E}\perp\mathbf{c}$ and $\mathbf{E}\|\mathbf{c}$ polarization SPV spectra of Cu_2ZnSiS_4 at room temperature. The inset illustrates the plots of $(Vh\nu)^{1/2}$ vs $h\nu$ for $\mathbf{E}\perp\mathbf{c}$ and $\mathbf{E}\|\mathbf{c}$ polarization in the vicinity of the indirect band gap.

2.97 ± 0.02 eV and 3.07 ± 0.02 eV, respectively. The value of E_g^{ind} as determined from the absorption data for the unpolarized incident light lies between $E_{g\perp}^{ind}$ and $E_{g\mathrm{II}}^{ind}$. The obtained values of $E_{g\perp}^{ind}$ and $E_{g\mathrm{II}}^{ind}$ are slightly different to the previous published one derived from unpolarized measurements.[8]

The unpolarized, $\mathbf{E}\perp\mathbf{c}$ and $\mathbf{E}\|\mathbf{c}$ polarization PzR spectra of Cu_2ZnSiS_4 in the energy range 2.7/3.1 eV (unploarized/polarized) to 3.6 eV are shown in Figs. 3(a)–3(c), respectively. As shown in Fig. 3(a), the oscillations on the lower-energy side are caused by the interference effect. The two dominant structures located between 3.20 and 3.55 eV are associated with band edge excitonic transitions from different origins and are assigned as $E_{\perp}^{ex}$ and $E_{\|}^{ex}$. As can be seen in Fig. 3(b), the $E_{\perp}^{ex}$ feature is observed in $\mathbf{E}\perp\mathbf{c}$ polarization, while the $E_{\|}^{ex}$ feature appears in $\mathbf{E}\|\mathbf{c}$ polarization [see Fig. 3(c)]. From the spectral characteristics of the PzR spectra, the features are most probably originating from the interband excitonic transitions. In order to determine the position of the transitions accurately, we have performed a theoretical lineshape fit for the PzR spectra to a functional form appropriate for excitonic transitions,[12–14]

$$\frac{\Delta R}{R}=\mathrm{Re}\sum_{j=1}A_j e^{i\Phi_j}(E-E_j+i\Gamma_j)^{-2}, \tag{2}$$

where A_j and Φ_j are the amplitude and phase of the lineshape, E_j and Γ_j are the energy and broadening parameter of the interband excitonic transitions, respectively. Shown by the solid curves in Figs. 3(a)–3(c) are the least-squares fits to Eq. (2). Arrows above the curves in Figs. 3(a)–3(c) show the energy positions of the two interband excitonic features, $E_{\perp}^{ex}$ and $E_{\|}^{ex}$. The obtained values of $E_{\perp}^{ex}$ and $E_{\|}^{ex}$ are 3.322 ± 0.005 eV and 3.408 ± 0.005 eV, respectively, and are listed in Table I. The unpolarized spectrum can be regarded as a random superposition of the spectra with $\mathbf{E}\perp\mathbf{c}$ and $\mathbf{E}\|\mathbf{c}$ polarizations. The energy difference between the low- and high-energy transitions represents the crystal-field splitting between two levels of the valence band. Shay *et al.*[15] reported the symmetries and splitting of the uppermost valence bands in orthorhombic $AgInS_2$ polarized electrolyte electroreflectance measurements on oriented crystals. The valence band splitting observed was explained by crystal-field splitting alone, neglecting any spin-orbit interaction. The results showed that the direct band edge transitions for $\mathbf{E}\|\mathbf{c}$ polarization is higher than that of $\mathbf{E}\perp\mathbf{c}$ ($\mathbf{E}\|\mathbf{a}$ or $\mathbf{E}\|\mathbf{b}$) polarization. Our experimental finding that the excitonic transition energy of $E_{\|}^{ex}$ feature observed at $\mathbf{E}\|\mathbf{c}$ polarization is 86 meV larger than that of $E_{\perp}^{ex}$ at $\mathbf{E}\perp\mathbf{c}$ polarization concurred well qualitatively with the previous report of orthorhombic $AgInS_2$.[15]

The normalized SPV spectra of Cu_2ZnSiS_4 taken with unpolarized, $\mathbf{E}\perp\mathbf{c}$ and $\mathbf{E}\|\mathbf{c}$ polarization in the vicinity of near band edge region are illustrated in Fig. 4. For clarity the curves are displaced. It can be seen that, similar to PzR, SPV behavior strongly depends on polarization of incident light: the low-energy feature is presented in $\mathbf{E}\perp\mathbf{c}$ polarization, while high-energy feature appears in $\mathbf{E}\|\mathbf{c}$ polarization and the two structures are both observed in the unpolarized spectrum. By comparing with the spectra obtained from PzR measurements, the observed SPV features are determined to be due to excitonic transitions. The energy values obtained from SPV spectra are $E_{\perp}^{ex}=3.32\pm0.01$ eV and $E_{\|}^{ex}=3.40\pm0.01$ eV and agree quite well with observed excitonic features of the PzR spectra as depicted in Fig. 3.

The SPV signal V is considered to be proportional to the absorption coefficient α in the region of the absorption edge caused by indirect optical transition.[16–18] We analyzed the SPV spectrum using the relation $(Vh\nu)^{1/2}$ versus photon energy $h\nu$. The indirect band edge transition energy could be obtained by extrapolating the linear part of the plot $(Vh\nu)^{1/2}$ versus $h\nu$ to zero. As shown in the inset of Fig. 4, the fit using $(Vh\nu)^{1/2}$ versus $h\nu$ yields a satisfactory result which agrees well with the indirect band edge transition character of Cu_2ZnSiS_4. The results reveal that Cu_2ZnSiS_4 is an indirect band gap semiconductor in which $\mathbf{E}\perp\mathbf{c}$ polarization exhibits a smaller band gap than that of $\mathbf{E}\|\mathbf{c}$ polarization. Errors for the fitted values may also result by fitting a slightly

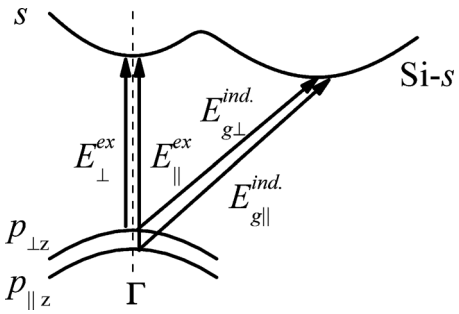

FIG. 5. A schematic representation of the plausible assignments for the observed optical transitions near band edge for Cu_2ZnSiS_4.

different range of the experimental data, thus errors of the order of ± 0.02 eV can be estimated for the deduction values of indirect band gap. The fitted values of $E_{g\perp}^{ind}$ and $E_{g\mathrm{II}}^{ind}$ are respectively, determined to be 2.99 ± 0.02 and 3.08 ± 0.02 eV and are also listed in Table I. The values of indirect transitions determined from SPV spectra are in good agreement with that determined from the absorption measurements.

In order to understand the obtained experimental results, a band diagram near band edge is needed. However, to the best of our knowledge, there are no prior studies of the electronic structure of Cu_2ZnSiS_4. A recent band structure calculation using a first-principles local-density-functional method on a family of I_2-II-IV-VI_4 quaternary chalcogenides semiconductors by Chen *et al.*[19] suggested that Cu_2ZnGeS_4 semiconductor with the primitive mixed Cu–Au structure has an indirect band gap with the lowest conduction band minimum (CBM) at A point and the valence band maximum (VBM) at Γ point of the Brillouin zone. The A point conduction bands of Cu_2ZnGeS_4 have three segregating states: one doubly degenerate state localized on CuS, a singly degenerate state localized on ZnS, and a singly degenerate state arising from GeS. The singly degenerate state arising from GeS is the CBM due to the much lower Ge *s* energy level. Assuming that Cu_2ZnSiS_4 is closely related to the Cu_2ZnGeS_4 compound, the identifications of the optical transitions observed in Cu_2ZnSiS_4 crystals can be done by adopting the results of the band structure calculations of Cu_2ZnGeS_4. Thus, the observed optical transitions near indirect band edge can be attributed to indirect transitions from the VBM at Γ point to the CBM at A, while excitonic transitions observed in the PzR and SPV spectra can be attributed to the direct transitions at Γ point. It should be noted that Cu_2ZnSiS_4 is crystallized in the wurtz-stannite structure which is different from that of the primitive mixed Cu–Au structure of Cu_2ZnGeS_4. Even the differences between both structures are small, the corresponding electronic structures could be quite different. In order to identify the origins of the observed near band edge transitions, the density function theory calculations on the wurtz-stannite structure of the studied compound is needed to be performed.

Adopting the band-structure calculation by Chen *et al.*,[19] a schematic representation of the plausible assignments for the observed optical transitions near band edge for Cu_2ZnSiS_4 is presented in Fig. 5. Construction of this schematic diagram at Γ point is based upon two assumptions. First, the conduction and valence bands are assumed to be dominated by *s*-like and *p*-like, respectively. It is referred from the crystal structure's tetrahedral bonding arrangement which arises from s-p^3 hybridization.[20,21] The degree of p-d hybridizations are assumed to be small and can be neglected. The *s*-like and *p*-like energy bands involved in the optical transitions shall have the same symmetry properties as the atomic functions *s*, $p_{\parallel z}$, and $p_{\perp z}$. The second assumption is that spin-orbit splitting is much less than the crystal-filed splitting and thus may be neglected. We infer this from the PzR and SPV spectra which exhibit one transition for $\mathbf{E} \perp \mathbf{c}$ and a distinctly higher transition for $\mathbf{E} \parallel \mathbf{c}$. The energy of the transition depends strongly on the orientation of the polarization with respect to the crystallographic directions. This suggests that the orbital angular momentum of the *p* states is sufficiently quenched to render the spin-orbit interaction negligible. Thus the splitting between the $\mathbf{E} \perp \mathbf{c}$ and $\mathbf{E} \parallel \mathbf{c}$ levels of the valence band shown in Fig. 5 is attributed solely to the orthorhombic crystalline symmetry of Cu_2ZnSiS_4 which described by the space group $Pmn2_1$.

IV. SUMMARY

In summary, room temperature polarization-dependent absorption, PzR and SPV measurements were carried out on the as grown basal plane of Cu_2ZnSiS_4 single crystals in the vicinity of the band edge region. The results revealed that Cu_2ZnSiS_4 is an indirect transition semiconductor with the indirect band gaps of 2.97 and 3.07 eV for light polarized with $\mathbf{E} \perp \mathbf{c}$ and $\mathbf{E} \parallel \mathbf{c}$ configurations, respectively. The polarization-dependent PzR and SPV spectra in the vicinity of the direct band gap reveal excitonic features $E_{\perp}^{ex}$ and $E_{\parallel}^{ex}$ at around 3.32 eV and 3.41 eV for $\mathbf{E} \perp \mathbf{c}$ and $\mathbf{E} \parallel \mathbf{c}$ polarizations, respectively. Base on the obtained results, a plausible band structure near band edge of Cu_2ZnSiS_4 is constructed. The splitting between the $\mathbf{E} \perp \mathbf{c}$ and $\mathbf{E} \parallel \mathbf{c}$ levels of the valence band is attributed to the orthorhombic crystalline symmetry of Cu_2ZnSiS_4 as described by the space group $Pmn2_1$.

ACKNOWLEDGMENTS

The authors acknowledge the support of National Science Council of Taiwan under Project Nos. NSC 098-2811-E-011-019, 97-2112-M-011-001-MY3, and 98-2221-E-011-015-MY2.

[1] R. Nitsche, D. F. Sargent, and P. Wild, J. Cryst. Growth **1**, 52 (1967).
[2] W. Schafer and R. Nitsche, Mater. Res. Bull. **9**, 645 (1974).
[3] L. Guen, M. S. Glausinger, and A. Wold, Mater. Res. Bull. **14**, 463 (1979).
[4] J. W. Lekse, M. A. Moreau, K. L. McNerny, J. Yeon, P. S. Halasyamani, and J. A. Aitken, Inorg. Chem. **48**, 7516 (2009).
[5] J. W. Lekse, B. M. Leverett, C. H. Lake, and J. A. Aitken, J. Solid State Chem. **181**, 3217 (2008).
[6] T. Oike and T. Iwasaki, AH01L2915FI, http://www.faqs.org/patents/app/20080303035#ixzz0iW8PX6KV
[7] D. M. Schleich and A. Wold, Mater. Res. Bull. **12**, 111 (1977).
[8] G. Q. Yao, H. S. Shen, E. D. Honig, R. Kershaw, K. Dwight, and A. Wold, Solid State Ionics **24**, 249 (1987).
[9] J. S. Blakemore and K. C. Nomura, Phys. Rev. **127**, 1024 (1962).
[10] D. L. Greenaway and R. Nitsche, J. Phys. Chem. Solids **26**, 1445 (1965).
[11] J. I. Pankove, *Optical Properties in Semiconductors* (Dover, New York, 1975), pp. 36–38.
[12] Y. S. Huang and F. H. Pollak, Phys. Status Solidi A **202**, 1193 (2005).

[13]D. E. Aspnes, in *Handbook of Semiconductors*, edited by M. Balkanski (North-Holland, Amsterdam, 1980), Vol. 2, p. 109.
[14]F. H. Pollak and H. Shen, Mater. Sci. Eng. R. **10**, xv (1993).
[15]J. L. Shay, B. Tell, L. M. Schiavone, H. M. Kasper, and F. Thiel, Phys. Rev. B **9**, 1719 (1974).
[16]L. Kronik and Y. Shapira, Surf. Sci. Rep. **37**, 1 (1999).
[17]D. Gal, Y. Mastai, G. Hodes, and L. Kronik, J. Appl. Phys. **86**, 5573 (1999).
[18]H. P. Hsu, P. Y. Wu, Y. S. Huang, S. Sanorpim, K. K. Tiong, R. Katayama, and K. Onabe, J. Phys.: Condens. Matter **19**, 096009 (2007).
[19]S. Chen, H. G. Gong, A. Walsh, and S. H. Wei, Phys. Rev. B **79**, 165211 (2009).
[20]O. W. Shih, R. L. Aggarwal, T. Q. Vu, Y. Shapira, K. Doverspike, R. N. Kershaw, K. Dwight, and A. Wold, Phys. Rev. B **45**, 14025 (1992).
[21]E. Parthé, *Crystal Chemistry of Tetrahedral Structures* (Gordon and Breach, New York, 1964).